National Aeronautics and Space Administration



Understanding How Molecular Hydrogen Impacts the Total Dose and Dose Rate Response of Linear Bipolar Circuits

Philippe Adell
Bernard Rax
Steve McClure
Jet Propulsion Laboratory, Pasadena, California

Hugh Barnaby
Jie Chen
Arizona State University, Tempe, Arizona

Ron Pease
RLP Research, Los Lunas, New Mexico

Jet Propulsion Laboratory
California Institute of Technology
Pasadena, California

JPL Publication 09-05 2/09

National Aeronautics and Space Administration



Understanding How Molecular Hydrogen Impacts the Total Dose and Dose Rate Response of Linear Bipolar Circuits

NASA Electronic Parts and Packaging (NEPP) Program
Office of Safety and Mission Assurance

Philippe Adell
Bernard Rax
Steve McClure
Jet Propulsion Laboratory, Pasadena, CA

Hugh Barnaby
Jie Chen
Arizona State University, Tempe, Arizona

Ron Pease
RLP Research, Los Lunas, New Mexico

NASA WBS: 939904.01.11.30
JPL Project Number: 103982
Task Number: 03.04.04

Jet Propulsion Laboratory
4800 Oak Grove Drive
Pasadena, CA 91109

http://nepp.nasa.gov

This research was carried out at the Jet Propulsion Laboratory, California Institute of Technology, and was sponsored by the National Aeronautics and Space Administration Electronic parts and Packaging (NEPP) program.

Reference herein to any specific commercial product, process, or service by trade name, trademark, manufacturer, or otherwise, does not constitute or imply its endorsement by the United States Government, the (name of sponsor if it is not a federal government organization), or the Jet Propulsion Laboratory, California Institute of Technology.

Copyright 2008. California Institute of Technology. Government sponsorship acknowledged.

ABSTRACT

Recent Enhanced Low Dose Rate Sensitivity (ELDRS) investigations carried out by RLP Research, Arizona State University (ASU) and Jet Propulsion Laboratory (JPL) have shown significant differences in the degradation of bipolar micro-circuits with total dose in the presence of molecular hydrogen (H_2) in packages. This has a significant impact on radiation hardness assurance and opens up opportunities to improve device performance.

The general objectives of this program are to:

1. Determine the extent to which hydrogen contamination affects the total dose and dose rate response of linear bipolar circuits;
2. Develop a model that will enable the prediction of high dose rate (HDR) and low dose rate (LDR) response asymptotes and transition dose rates as a function of total dose, temperature, pressurized hydrogen, defect precursors, and other process dependent variables;
3. Explore the possibility of an accelerated hardness assurance method and possible hardening approaches; and
4. Extend the work to other technologies that have total dose response affected by hydrogen contamination.

In this document, we experimentally demonstrate with test transistors and circuits that hydrogen is correlated with ELDRS in bipolar linear circuits. We show that the amount of hydrogen determines: 1) the total dose response versus dose rate and 2) the transition dose rates between the high and low dose rate responses. The experimental results are supported with a steady state drift/diffusion analytical model as well as modeling calculations using COMSOL Multiphysics.

SUMMARY OF FY07 EFFORT

Hydrogen (H_2) is ubiquitous in today's semiconductor integrated circuit (IC) fabrication and packaging processes [1]. During IC fabrication, H_2 is present in wafer cleaning procedures, film depositions, etches, high and low temperature anneals, and an assortment of other processes. During IC packaging, it is introduced during die attach and by forming gases during packaging processes [2]. H_2 can outgas from grain boundaries or structural imperfections in iron-nickel alloy (kovar, Alloy42) lead frame material. Electro-plated metal components such as plated gold or nickel films are major sources of dissolved hydrogen. Moisture is often present and results from the absorption or adsorption of H_2O on the internal surfaces of the package prior to sealing or from the sealing gas itself that is moist.

Solutions to hydrogen contamination have been reported and include thermal treatment, the use of package materials with low hydrogen absorption, a change of barrier materials in gates, and the use of hydrogen getters inside the packaging to absorb the hydrogen. However, there is no clear guideline or limit as to what level of hydrogen might be considered acceptable in sealed packages. The military standard test method for internal gas analysis, MIL-STD-883 Test Method 1018, was designed to look for moisture and not hydrogen or other gas impurities. There is no specification limit out on H_2. This lack of specification introduces another unknown when dealing with the radiation response of commercial linear bipolar devices. As it will be shown in this report, the commercial linear bipolar devices' total ionizing dose (TID) response and sensitivity to enhance low dose rate sensitivity (ELDRS) is affected.

In FY07, we reported on the impact of hydrogen contamination on the total dose response of linear circuits. A general investigation was performed on a selection of key parts from different manufacturers that all exhibit ELDRS as well as differences in the total dose degradation with bias conditions and dose rates. Residual gas analyses (RGAs) and die passivation analyses were performed on these devices. The results of this study clearly indicated that there is a correlation between ***packaging characteristics and hydrogen content***. The results suggested that by only looking at the package characteristics (ceramic package with or without gold plating, with or without kovar lids, can package, passivation layers, etc…), it is possible to evaluate which category of device is likely to have a non-negligible amount of hydrogen (~0.5 to 3%) in the package and which, consequently, might be sensitive to total-dose and low-dose-rate enhancement. We showed that 1) devices in cans package exhibit low amounts of hydrogen; 2) ceramic frit glass devices show negligible amounts of hydrogen; 3) parts that also have a nitride passivation layer do not show a significant quantity of hydrogen, though there is not necessarily a correlation here; and 4) both cases of ELDRS and non-ELDRS were found for nitride coated devices. While silicon nitride is a very good barrier to hydrogen diffusion, the deposition processes are known to introduce hydrogen into device passivation layers. Thus, we believe it is critical to investigate the mechanisms of hydrogen absorbtion/desorption in nitride passivations.

In addition, two parts, the HSYE-117RH linear voltage regulator from Intersil and the AD590 temperature transducer from Analog Devices, were identified as parts showing a significant amount of hydrogen (~0.6 - 3 %) in their package. Further experiments were conducted to identify the relationship between ***hydrogen content and total dose***

response. Twelve screened space-qualified AD590s were irradiated at both high and low dose rates unbiased with all leads grounded. Three flatpacks (with 0.4 - 1% H_2) and three cans (~0% H_2) were irradiated up to 30 krad with a low dose rate (LDR) of 0.01 rad/s. Three flatpacks and three cans were irradiated up to 100 krad with a high dose rate (HDR) of 25 rad/s. In addition, two parts of the HYSE-117RH (~3 % H_2) from the same wafer lot were irradiated unbiased at a dose rate of 0.05 rad/s. One part was opened for more than a week to release the hydrogen content. The results led to the following conclusions: 1) flatpack devices degrade much more at both low and high dose rates compared to the cans due to hydrogen contamination; 2) devices in the high dose and low dose rate case degrade more as the amount of hydrogen content increases; 3) cans devices can be made to degrade similar to the flatpack when the die is exposed to H_2; 4) the devices in the high and low dose rate case degrade more as the amount of hydrogen content increases; and 5) parts that have an oxide passivation are more affected by molecular hydrogen (H_2) in packages. The results clearly confirmed the correlation between ***total dose response, packaging, and hydrogen contamination***. For the HSYE-117, the same trends were observed but more experiments were needed with more devices to confirm. Current work with Intersil is ongoing and consists of evaluating twelve devices in three different packages (with different concentrations of H_2) and comparing the HDR and LDR behavior. Preliminary results show the same impact of hydrogen on the total dose response and will be presented early in FY09.

In order to explain the underlying mechanisms that relate to the role of ***hydrogen contamination in the total dose response of linear bipolar microcircuits,*** additional work was performed at Arizona State University. A combination of modeling and experiments were conducted on gated lateral pnp (GLPNP) devices fabricated at National Semiconductor. These devices were specifically designed to study ELDRS. Experimental results showed a monotonic increase in radiation-induced interface traps as well as oxide-trapped charge with increasing molecular hydrogen concentration in the ambient during irradiations. Using chemical kinetics and previously developed models for interface trap formation, a first order model was proposed to describe the relationship between interface trap formation and excess molecular hydrogen concentration in gaseous ambient during radiation exposure. This model provided an excellent fit to the data obtained from the experiments.

In FY08, we focused our effort by providing a better understanding on how hydrogen impacts the ***total dose and dose rate response of linear bipolar circuits and its correlation with ELDRS***. Test circuits and transistors designed for this particular purpose were available. A wide range of irradiation was performed at different dose rates and at different hydrogen concentrations. Experimental results are supported with a model of the basic processes that describe the observed dependence.

TABLE OF CONTENTS

1.0 INTRODUCTION 1
2.0 THE EFFECTS OF HYDROGEN ON THE ENHANCED LOW DOSE RATE SENSITIVITY (ELDRS) 3
2.1 Experimental Results – GLPNPs 4
2.2 Experimental Results – LM193 7
2.3 Conclusion 9
3.0 MODELING 10
3.1 Effect of H2 on Nit Formation 10
3.2 Modeling Effect of Hydrogen on TID Response 11
3.3 Modeling ELDRS and Effect of Hydrogen on ELDRS 15
3.4 Simulation Results Using COMSOL 19
4.0 CONCLUSIONS AND IMPLICATIONS 21
5.0 REFERENCES 23

TABLE OF FIGURES

Fig 1. MPTB experiments comparing space data with ground Co60 data. 2
Fig 2. Gated lpnp 2D cross section and layout. 3
Fig. 3. Picture of glass tubes used by JPL for exposure in H_2. 4
Fig. 4. Extracted value of increase in N_{it} versus hydrogen concentration for GLPNPs at 30 krad for irradiation at several dose rates. 5
Fig 5. N_{it} versus dose rate for irradiation to 30 krad for the GLPNPs with p-glass. Lines are hypothetical curves to guide the eye. 6
Fig. 6. Increase in base current at a base-emitter voltage of 0.5 V versus dose rate for irradiation to 30 krad for the GLPNPs with p-glass. Lines are hypothetical curves to guide the eye. 6
Fig. 7. Input bias current versus dose at several dose rates for the LM193 with standard passivation and no external hydrogen. 7
Fig. 8. Change in input bias current versus dose for irradiation at 25 rad/s for parts with nitride removed (p-glass intact) and different H_2 concentrations. 8
Fig. 9. Change in input bias current versus dose for irradiation at 0.1 rad/s for parts with nitride removed (p-glass intact) and different H_2 concentrations 8
Fig. 10. Increase in input bias current versus dose rate for irradiation to 10 krad for the LM193s with p-glass and different H_2 and for nitride with no H_2. Lines are hypothetical curves to guide the eye. 9
Fig. 11. Estimated radiation-induced interface trap buildup versus molecular hydrogen concentration in the oxide at 30krad(SiO_2). 10
Fig. 12. Estimated radiation-induced oxide-trapped-charge (N_{ot}) buildup versus molecular hydrogen concentration in the oxide plotted with the N_{it} data. 11
Fig. 13. Cartoon shows the reaction between molecular hydrogen and vacancy defects in the oxide. 13
Fig. 14. Comsol Simulation versus ASU Data on the effect of H_2. 15

Fig. 15. Simulations of ELDRS model incorporating e/h recombination as a core mechanism. The simulations were performed with several applied bias conditions to show the bias dependence of ELDRS. 17
Fig. 16. The dose rate experimental data showing bias dependence of ELDRS response obtained from lateral pnp transistors. 17
Fig. 17. Conception of core processes in a device exhibiting ELDRS with low hydrogen concentration. 18
Fig. 18. Conception of core processes in a device exhibiting ELDRS with high hydrogen concentration. 19
Fig. 19. Simulation of the effect of hydrogen on ELDRS response: right shift of transition dose rates and increase of low dose rate saturation limit. 20
Fig. 20. Comparison of post irradiation N_{it} for a glpnp irradiated to 30 krad(Si) at 20 mrad(Si)/s in air to irradiation at 100 rad(Si)/s in 100% H_2 (left) and delta Ib of an LM193 to 10 krad(Si) at 2 mrad(Si)/s in air to irradiation at 100 rad(Si)/s in 100% H_2 (right). 22

1.0 INTRODUCTION

Bipolar linear circuits are in common use in space systems where they are exposed to ionizing radiation at very low dose rates. It has been demonstrated that many bipolar linear circuits exhibit a "true" dose rate effect that has become commonly known as enhanced low dose rate sensitivity (ELDRS) [3]–[6]. ELDRS is characterized by a low dose rate enhancement factor (EF) that is the ratio of the parametric degradation at a low dose rate (LDR) to the degradation at a high dose rate (HDR) for a fixed dose. EF is not a universal number and varies for different part types and for different parameters within the same part. This approach to characterizing the dose rate response of bipolar devices and circuits as an enhancement factor versus dose rate was first used by Johnston, et al. [5].

For space applications, it is usually hard to identify system malfunctions related to ELDRS because failures are usually parametric and not functional. Design margins are often high and circuits are often not "suspect" if they passed ground test at HDR. Most devices and circuits that exhibit ELDRS show a response that is characterized by an enhancement factor of one at high dose rate (usually >100 rad/s) and an enhancement factor that reaches an asymptote between 2 and ~100 at low dose rate (usually ~10 mrad/s or less).

To demonstrate beyond question that ELDRS is a real effect in space, an experiment was run on the Microelectronics and Photonics Testbed (MPTB) program using the LM139 quad comparator. The experiment ran for about seven years, and the parts accumulated ~45 krad(Si), with most of the dose received in the one hour flight through the radiation belts during each 12-hour orbit [7]–[8]. This corresponds to an average dose rate of about 2.5 mrad/s. The results for the LM139 are shown in Fig. 1, comparing various ground tests at constant dose rate to the space results. Although the space environment consists of protons and electrons of various energies and widely changing dose rates, the degradation falls between the degradation at a constant dose rate of 1 mrad(Si)/s and 10 mrad(Si)/s using Co-60. The results at 10 and 100 rad(Si)/s show much less degradation than in space and the elevated temperature irradiation at 100°C and 1 rad(Si)/s falls in between. Note that the input bias current that started at 25 nA reached 400 nA, which could be a problem for some system applications. The pre-irradiation specification limit for this parameter is 100 nA.

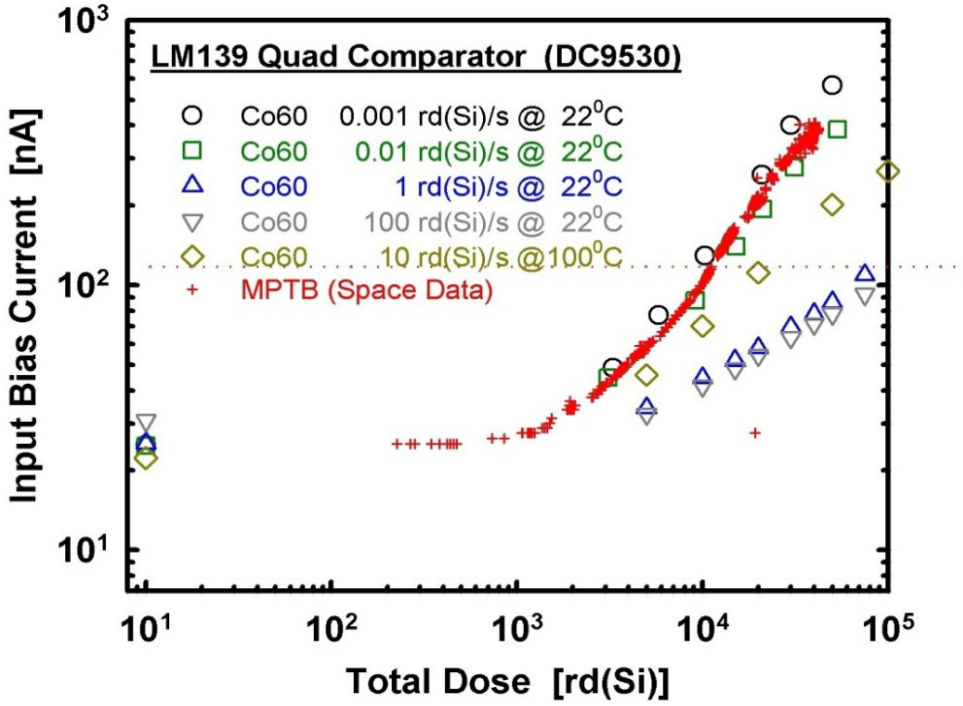


Fig 1. MPTB experiments comparing space data with ground Co60 data.

The total dose and dose rate responses of bipolar circuits depend on a number of factors: final passivation (or processing tools) [9]–[11], pre irradiation thermal stresses during burn-in or packaging [12], and the amount of an external source of hydrogen, e.g., in the sealed package [13]–[15]. However, the exact factors that determine the maximum enhancement factor and the dose rate where the transition between high and low dose rate response occurs have never been determined precisely. We define the transition dose rates as the region where the enhancement between the high dose rate and low dose rate occurs. It does not need to be quantified, but it is a good signature of the total dose behavior of a particular part.

The largest low dose rate enhancement factors that have been observed occur in bipolar linear circuits that incorporate lateral and substrate pnp transistors [9]. For these circuits, the primary degradation mechanism is an increase in the base current resulting from an increase of interface traps (N_{it}). Most models for radiation-induced N_{it} buildup maintain that positively charged hydrogen (protons), released in the oxide as a result of ionizing radiation processes, transport to the interface and react at H-passivated bonds to create traps at Si/SiO_2 interfaces. In FY07, we showed that a small amount of hydrogen can have a significant effect on low dose rate response and that 100% hydrogen can cause significant degradation at high and low doses rate [14].

In this work, we show that the amount of hydrogen from an external source determines the transition dose rate for the low dose rate enhancement as well as the maximum value of the enhancement factor. This implies that there is a direct correlation between the amount of hydrogen in the critical base oxide and ELDRS. These results are supported with a model of the basic processes that describe the observed dependence.

2.0 THE EFFECTS OF HYDROGEN ON THE ENHANCED LOW DOSE RATE SENSITIVITY (ELDRS)

Both bipolar linear test transistors and circuits were characterized in the course of this investigation. The test transistors, as shown on Fig 2., are part of an ELDRS test chip from a single wafer lot designed to study the buildup of oxide-trapped charge and interface traps with the National Semiconductor Corporation (NSC) linear circuit technology and was fabricated in Arlington, Texas [9]. This special wafer lot was fabricated with several different combinations of the final passivation [9]. The samples were packaged by Golden Altos in 14 lead dual in-line packages (DIPs) with sealed KOVAR lids. Sealed KOVAR lid packages were analyzed as received with residual gas analysis (RGA) and shown to have ~1.2 to 1.4% H_2 in the cavity. The test chip includes gated lateral pnp transistors (GLPNPs) as well as an npn transistor and a non-gated lateral pnp transistor. The gated lateral pnp transistor is used to separately measure radiation-induced increases in oxide trapped charge (ΔN_{ot}) and interface trap (ΔN_{it}) densities [9].

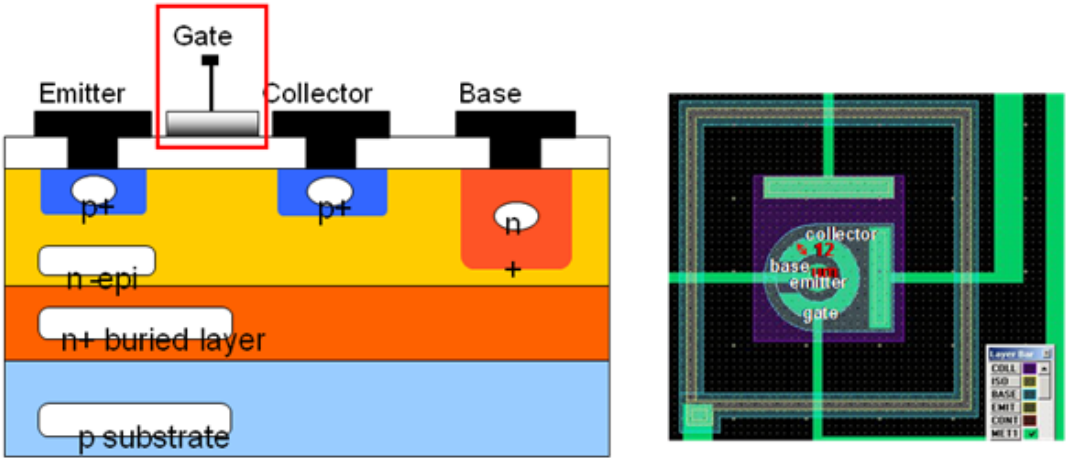


Fig 2. Gated lpnp 2D cross section and layout.

The circuit characterized in this study is an NSC LM193 dual voltage comparator. The LM193 is a dual version of the well characterized LM139 quad comparator and has the same circuit design and layout, utilizing substrate and lateral pnp transistors in the input stage circuit. The LM193 devices are from a single date code lot (date code 0551) and were purchased as commercial parts. They are packaged in 8-pin dual in-line ceramic packages with sealed ceramic lids and have a standard final passivation of nitride over p-glass. An RGA showed the presence of < 0.01% H_2 in the package cavity. Thirty of the parts had the lid removed and were subjected to a CF_4 / O_2 plasma etch (150 mTorr CF_4, 50 mTorr O_2, 125 Watt RF for three minutes) to remove the top nitride layer, leaving the p-glass passivation. The nitride is removed because it is a barrier to hydrogen.

The irradiations were carried out at Arizona State University (ASU) in a Gammacell 220 Co-60 source and at Jet Propulsion Labs (JPL) in a Shepherd 81 Co-60 irradiator. All irradiations were conducted with all leads shorted and grounded. The irradiations in 1% and 100% H_2 were conducted with the parts inside a sealed glass tube that was evacuated and then filled with H_2 to the appropriate partial pressure. The vacuum level in each tube before being soaked by H_2 was 10^{-5} torr. A picture of the glass tubes used by JPL for the H_2 exposures is shown in Fig. 3.

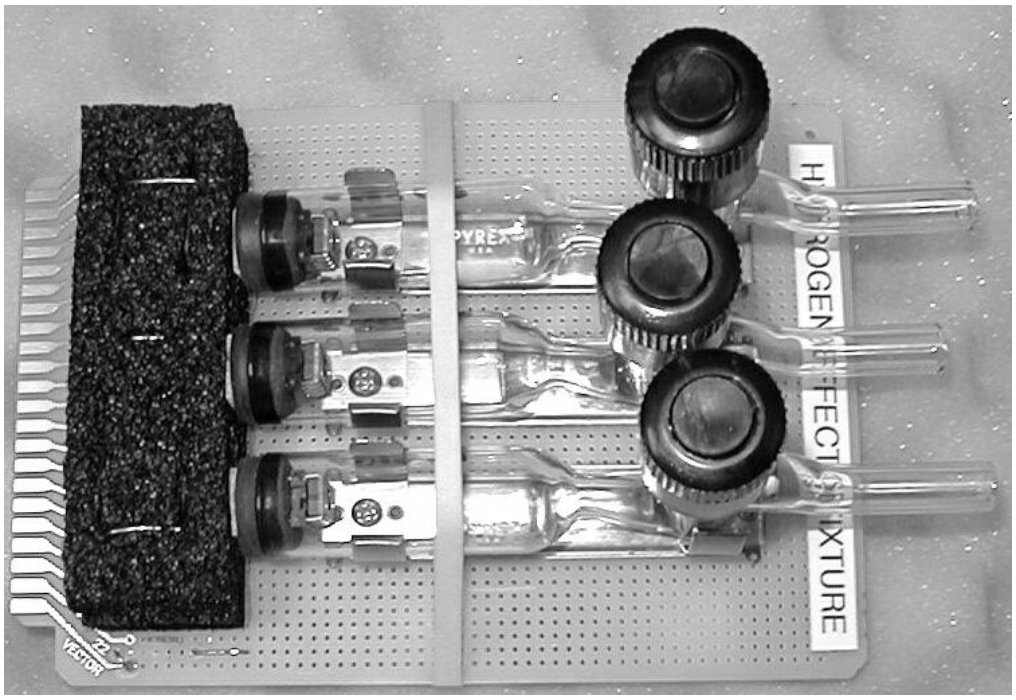


Fig. 3. Picture of glass tubes used by JPL for exposure in H_2.

All of the parts in the glass tube were soaked in the H_2 gas ambient for a minimum of 48 hours before irradiation to allow the H_2 to penetrate the p-glass. The range of dose rates used varied from 2 mrad/s to 100 rad/s, while the maximum total dose varied from ~8 krad to 100 krad. The electrical measurements on the ELDRS test chip GLPNPs were taken with an HP4156 parametric analyzer and consisted of base current versus gate voltage for fixed V_{be} and V_{cb} and emitter (drain) current versus gate voltage for the device biased as a pMOS transistor [9]. The LM193 was characterized for all dc specification parameters using an LTS2020 linear circuit tester.

2.1 Experimental Results – GLPNPs

The experiments on the GLPNPs were performed both at ASU and JPL sources. Data were taken on the transistors in the sealed KOVAR lid packages (i.e., ~1.2 to 1.4% H_2 in the cavity), in air (with the lid off), and in the glass tube at 100% H_2 over a range of dose rates from 0.02 to 100 rad/s, all to a total dose of 30 krad. The sample size was three for each set of conditions. For each data set the value of N_{it} was extracted using the method discussed in [9]. Fig. 4 is a plot of the average increase in N_{it} versus the hydrogen concentration, including data taken in an earlier experiment by NAVSEA Crane at 20 mrad/s [9]. The error for each data point is within the symbol. It is clear that the value of N_{it} increases with the amount of externally applied H_2 and with decreasing dose rate. With 100% H_2 (atmospheric pressure), N_{it} at high dose rate is greater than at low dose rate for parts with no externally applied H_2.

In Fig. 5 we show the data for the increase in N_{it} (average of three samples) versus the dose rate for irradiation to 30 krad. The lines are a guide for the eye and suggested hypothetical curves based on previous experimental data [26, 27] that show saturation at very low dose rates, current ELDRS models [18, 20, 24], and the Hydrogen/ELDRS model presented in this document. There are two clear trends in the data. As the H_2

concentration is increased, the maximum N_{it} value at low dose rate increases and the transition between high dose rate and low dose rate response moves to higher dose rate. The highest dose rate that could be achieved with the available sources was 100 rad/s. At this dose rate, we did not see a significant decrease in the N_{it} value of the 100% H_2 sample. This suggests that N_{it} value will decrease at higher dose rates.

A similar trend is seen for the average increase in base current for a base-emitter voltage of 0.5 V and a gate bias of 0 V, as shown in Fig. 6. Again the error for each data point is within the symbol. The correlation between the increase in N_{it} and the increase in base current establishes the dependence of lpnp base current on the increased interface trap density. We note that the input bias current of the LM193 is primarily the base current of a lateral pnp transistor in the input circuitry and, therefore, would also be expected to depend on the increase in N_{it}.

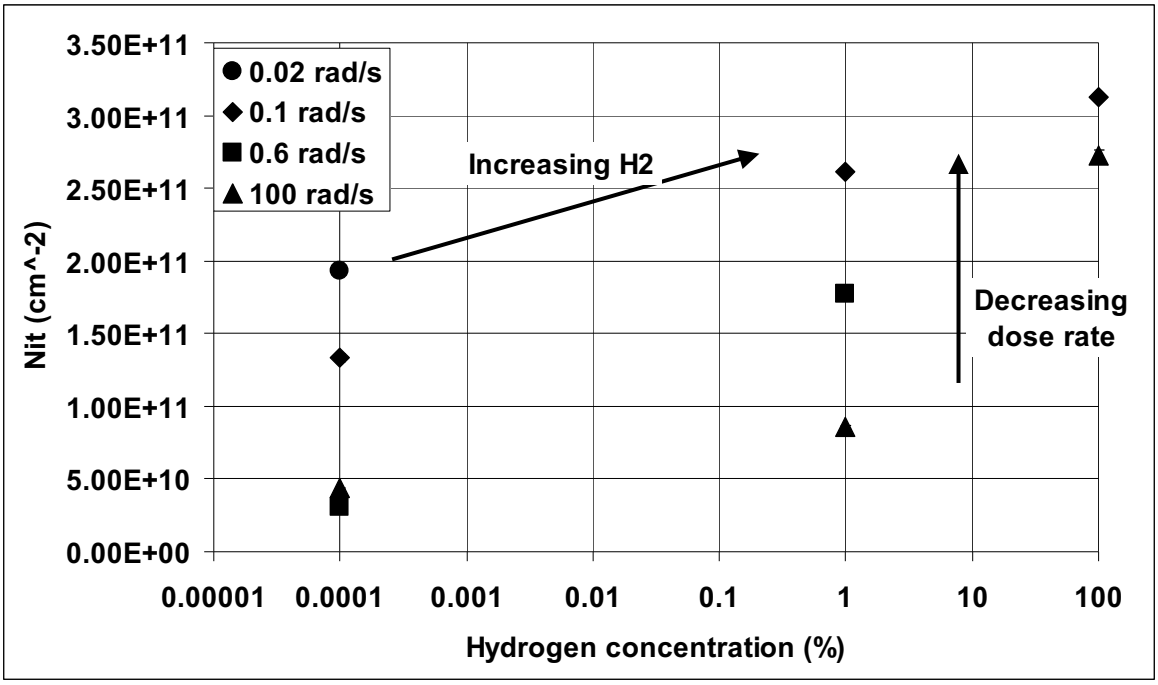


Fig. 4. Extracted value of increase in N_{it} versus hydrogen concentration for GLPNPs at 30 krad for irradiation at several dose rates.

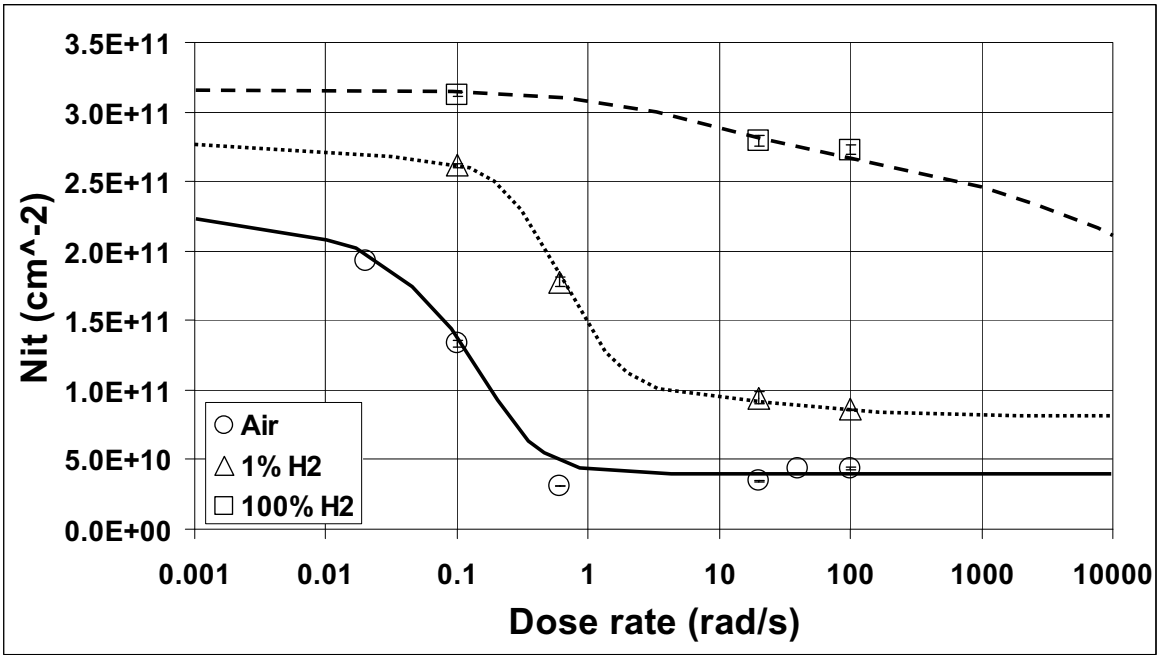


Fig 5. N_{it} versus dose rate for irradiation to 30 krad for the GLPNPs with p-glass. Lines are hypothetical curves to guide the eye.

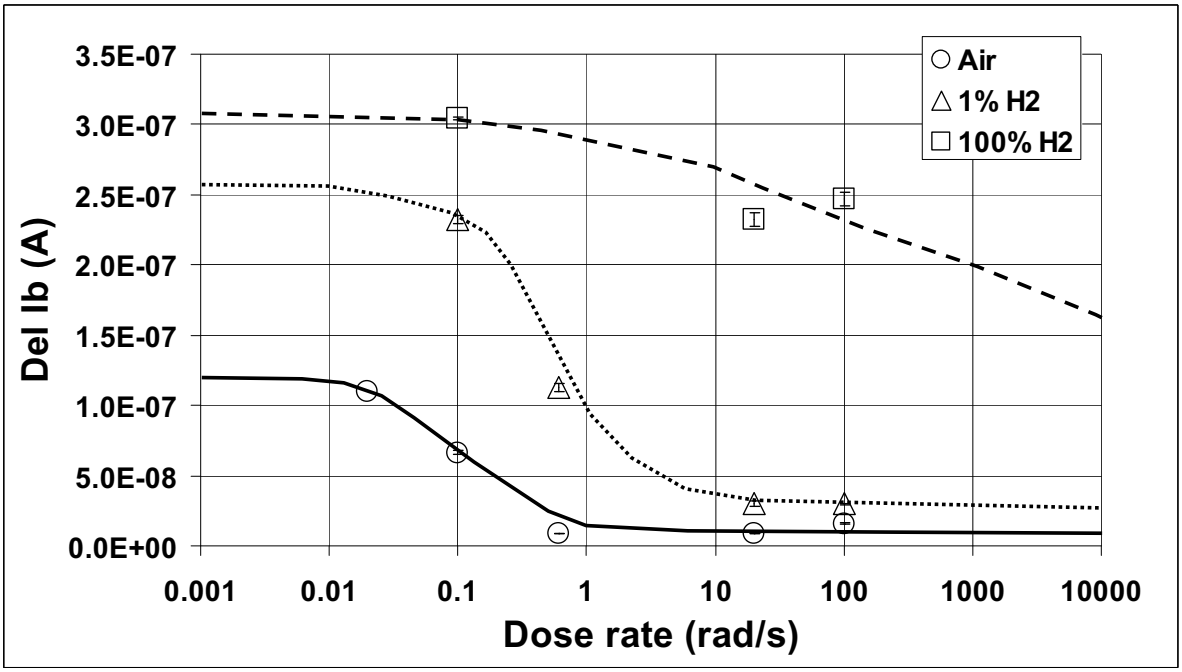


Fig. 6. Increase in base current at a base-emitter voltage of 0.5 V versus dose rate for irradiation to 30 krad for the GLPNPs with p-glass. Lines are hypothetical curves to guide the eye.

2.2 Experimental Results – LM193

The NSC LM193s were irradiated at JPL using their Shepherd 484 Co-60 irradiator. The initial testing was performed on the as-purchased parts over a range of dose rates from 2 mrad/s to 25 rad/s. A plot of the increase in input bias current (Ib) versus dose for the various dose rates is shown in Fig. 7. These data show that, between 5 mrad/s and 2 mrad/s, the degradation is still increasing, an effect that is not often seen in ELDRS parts but was reported for several parts in [15].

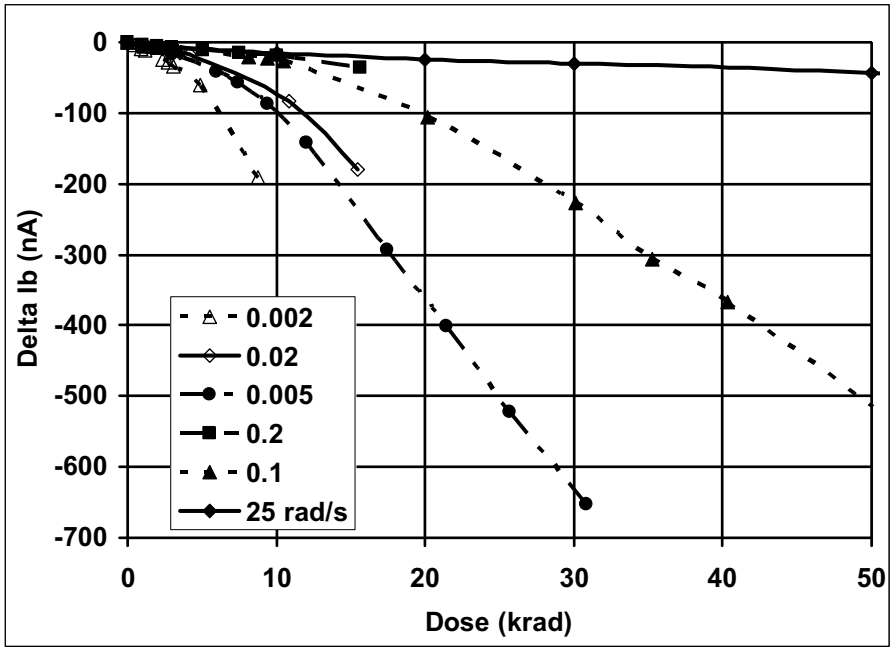


Fig. 7. Input bias current versus dose at several dose rates for the LM193 with standard passivation and no external hydrogen.

Additional experiments were performed on parts that were de-lidded and had the nitride removed by plasma etching. These parts were exposed at a variety of dose rates for exposure in air (~0% H_2) and in a glass tube with 1% and 100% H_2. Fig. 8 shows the results for exposure at 25 rad/s and Fig. 9 shows the results for exposure at 0.2 rad/s. It is clear that as the amount of H_2 is increased the degradation becomes more severe. In comparing Figs. 8 and 9, it is determined that the parts demonstrate ELDRS.

In Fig. 10, we plot for each sample the absolute value of delta Ib for both the as-purchased parts (virgin-0%H_2) and the parts with the nitride removed and exposed to different concentrations of H_2 versus dose rate for exposure to 10 krad. Lines are hypothetical curves to guide the eye. Again we see the same trend as with the GLPNPs. The maximum value of delta Ib increases with increasing H_2, and the transition between high and low dose rate responses moves to high dose rates.

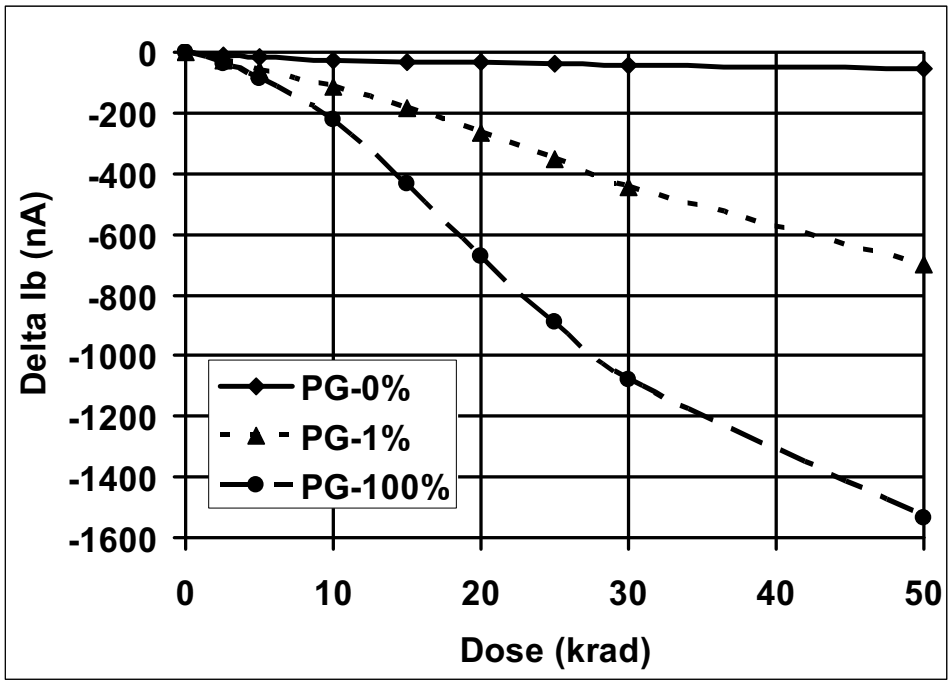


Fig. 8. Change in input bias current versus dose for irradiation at 25 rad/s for parts with nitride removed (p-glass intact) and different H_2 concentrations.

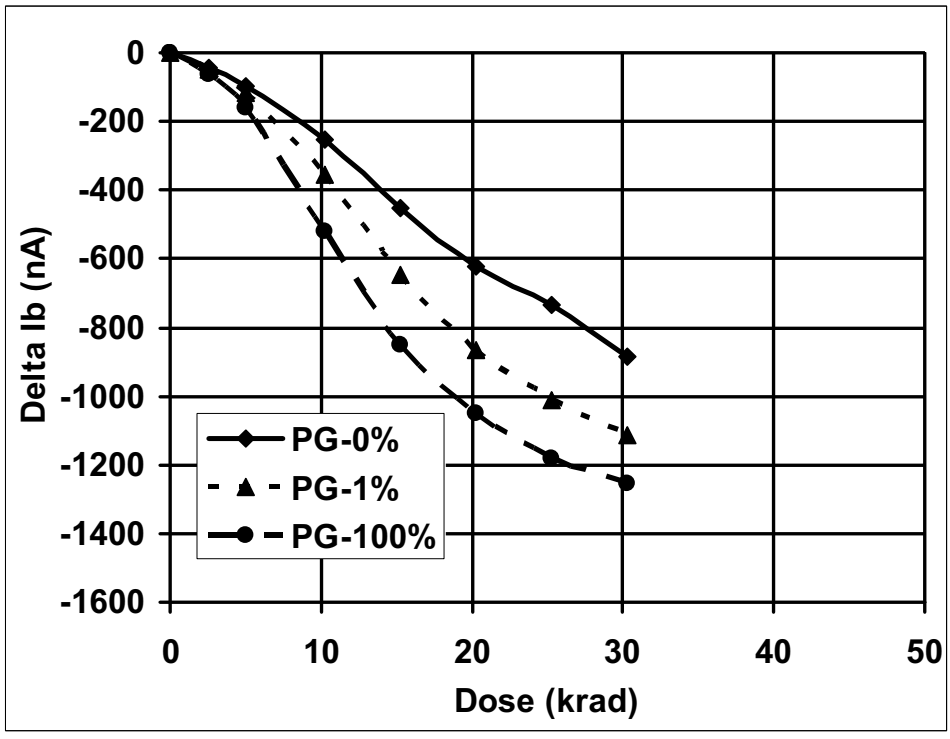


Fig. 9. Change in input bias current versus dose for irradiation at 0.1 rad/s for parts with nitride removed (p-glass intact) and different H_2 concentrations.

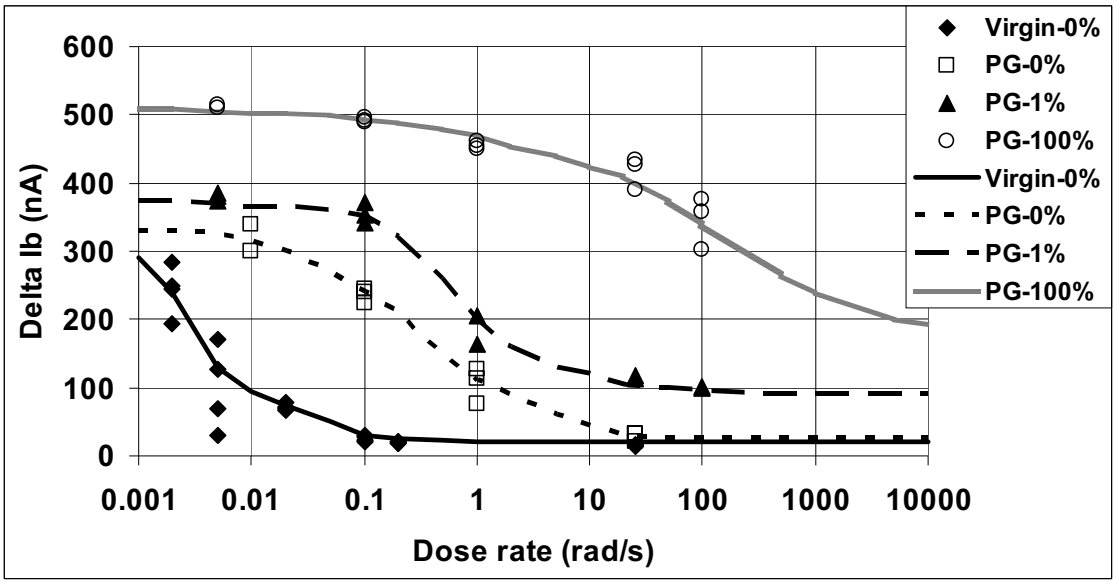


Fig. 10. Increase in input bias current versus dose rate for irradiation to 10 krad for the LM193s with p-glass and different H_2 and for nitride with no H_2. Lines are hypothetical curves to guide the eye.

2.3 Conclusion

Through these experiments we showed that:

1. Increasing H_2 concentration increases device total dose degradation for both HDR and LDR.
2. Exposure at high dose rate in 100 % H_2 causes more degradation than exposure in air at low dose rate.
3. The transition between high and low dose rate response moves to higher dose rate with increasing H_2.

3.0 MODELING

The experimental results shown in Figs. 3 and 10 illustrate the role of hydrogen in determining the total dose response and the low dose rate sensitivity of bipolar linear circuit technologies where the total dose response is dominated by the lateral and substrate pnp transistors. As the amount of hydrogen introduced into the base oxide is increased, we see two trends: 1) the degradation at low dose rate and high dose rate is increased and 2) the transition between high and low dose rate response moves to higher dose rates. To model these effects we use a steady state drift/diffusion analytical model as well as a 2-D modeling calculation using COMSOL Multiphysics.

3.1 Effect of H_2 on N_{it} Formation

We used the interface trap estimation method to plot the radiation induced N_{it} for the GLPNP devices [16]. Fig. 11 is the plot of interface trap density versus the hydrogen concentration after radiation exposure. In the figure, the extracted ΔN_{it} data are shown for experiments performed at both Crane and ASU. The concentration of H_2 molecules that permeate into the bipolar base oxide are approximated from volume percent (fraction of gas per unit volume) to volume density (molecules per unit volume) using Henry's Law.

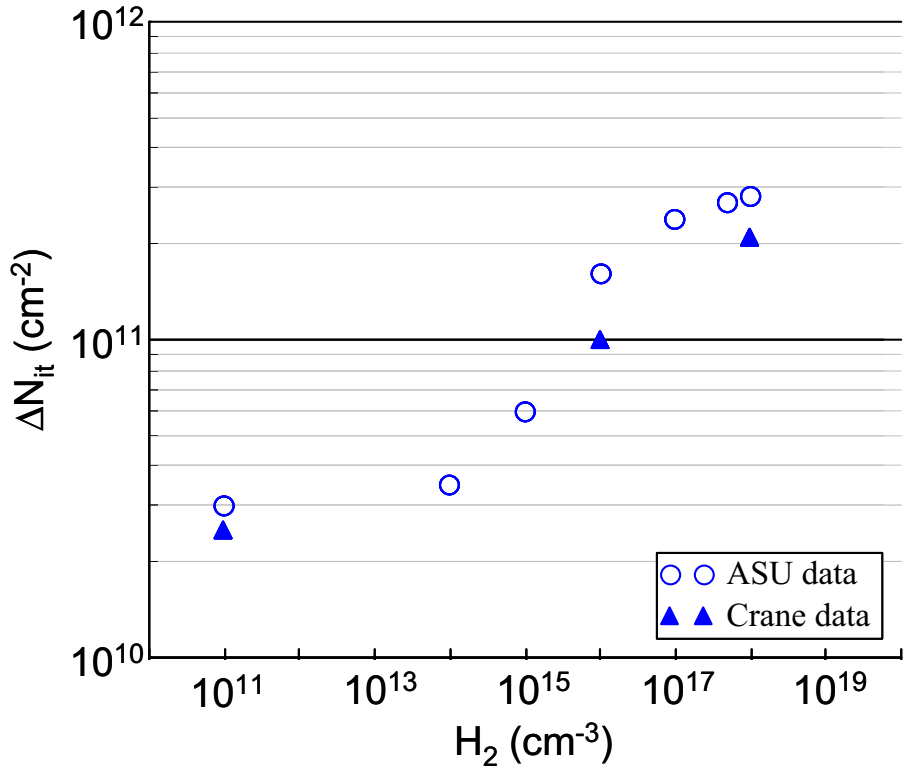


Fig. 11. Estimated radiation-induced interface trap buildup versus molecular hydrogen concentration in the oxide at 30krad(SiO_2).

$$N_{H_2,ox} = \kappa_{H_2,ox} P_{H_2} \tag{2}$$

where the solubility of H_2 in oxide, $\kappa_{H2,ox}$, is approximately 10^{18} cm^{-3} atm^{-1}, and P_{H2} is

the partial pressure of H_2 computed from volume percentage in the ambient. From the plot, one sees that the interface trap density changes the most between H_2 concentrations of 10^{14} cm^{-3} to 10^{17} cm^{-3}, and N_{it} buildup saturates at both high and low concentrations of H_2.

Using the sub-threshold extraction method [16], the amount of radiation-induced oxide trapped charge (ΔN_{ot}) was also extracted, shown in Fig. 12, along with extracted ΔN_{it} data. Like the ΔN_{it} data, the radiation-induced N_{ot} also increases with H_2 concentration and saturates at both high and low concentrations of H_2.

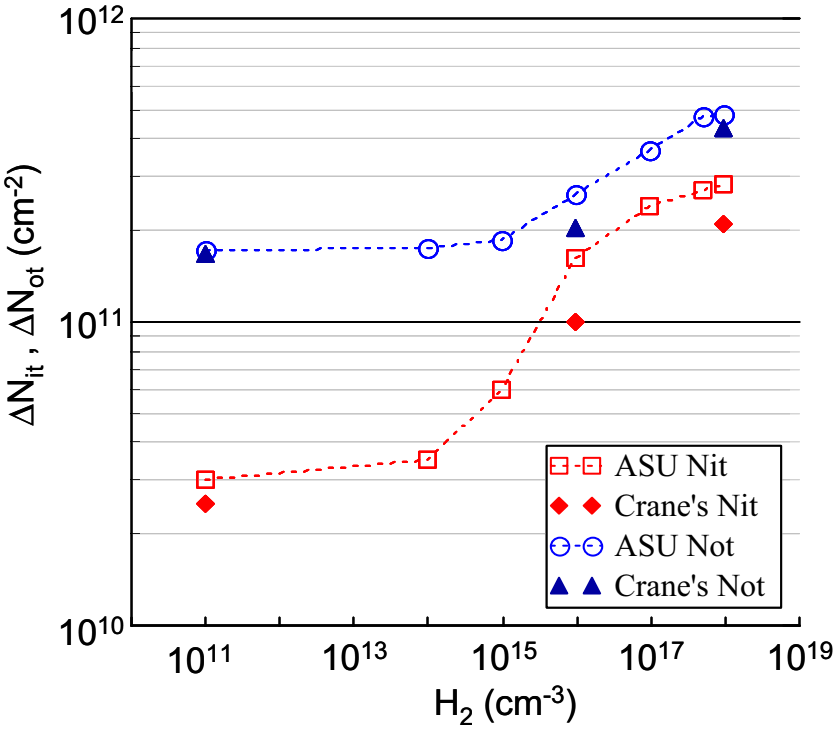


Fig. 12. Estimated radiation-induced oxide-trapped-charge (N_{ot}) buildup versus molecular hydrogen concentration in the oxide plotted with the N_{it} data.

In Figs. 11 and 12, though the general trends in the plots are similar, there are slight differences in the Crane and ASU experimental data. This is most likely due to the differences in pre-radiation characteristics, radiation source dosimetry, doses rates, and/or characterization environments during the experiments.

3.2 Modeling Effect of Hydrogen on TID Response

One of the most widely accepted models for radiation-induced interface trap formation is the two-stage hydrogen transport model originally proposed by McLean [17] and later refined by Rashkeev in [18]. In the simplest description of the model, electron-hole pairs are generated by radiation in the oxide and, after surviving initial recombination, a fraction of holes transport through the oxide. Electrons either recombine or are swept away by the gate. The hole generation, recombination, and transport processes in the oxide can be coupled in the continuity equation:

$$\frac{\partial p}{\partial t} = \dot{D} k_g f_y - \frac{\partial f_p}{\partial x} . \tag{3}$$

In (3), p is the hole concentration (cm^{-3}), f_p is the hole flux ($cm^{-2}s^{-1}$), $\dot{D}$ is the radiation dose rate, k_g is the dose to concentration conversion factor, and f_y is the hole yield that describes the fraction of holes that survived initial recombination [18]. Based on data from biased irradiation experiments [19], radiation-induced interface trap formation depends on a positively charged species, which is universally accepted as protons (H^+). Generated from reactions with released holes during irradiation, H^+ transport to the Si/SiO_2 interface and react with H-passivated silicon dangling bonds (P_b centers) to form interface traps. Similar to Equation (3), the proton continuity equation can be expressed as,

$$\frac{\partial H^+}{\partial t} = N_{DH} \sigma_{DH} f_p - \frac{\partial f_{H^+}}{\partial x} , \tag{4}$$

where H^+ is the proton concentration (cm^{-3}), f_{H+} is the proton flux ($cm^{-2}s^{-1}$), N_{DH} is the concentration of hydrogen-containing defect centers (DH), and σ_{DH} is the capture cross-section of holes reacting with the DH centers (cm^2) [19]. The interface trap formation rate is related to proton flux though the equation,

$$\frac{\partial N_{it}}{\partial t} = (N_{Si-H} - N_{it}(t)) \sigma_{it} f_{H^+} - \frac{N_{it}(t)}{\tau_{it}} , \tag{5}$$

where N_{Si-H} is the surface concentration of passivated dangling bonds (cm^{-2}), σ_{it} is the proton capture cross-section (cm^2), and τ_{it} is the interface trap lifetime used here to account for N_{it} annealing [18].

Based on our experimental results and the model presented in [17–18], a model is proposed to describe interface trap formation as a function of the H_2 present during radiation exposure. In this model, molecular hydrogen reacts with process-related neutral oxide defects at room temperature prior to and during irradiations to form hydrogen complexes in the oxide. Though originally speculated as H_2 reacting with two separate neutral defects to form two hydrogen complexes, quantum mechanical calculations performed by Batyrev, et al., later suggested that the reaction below is more physically feasible [20],

$$H_2 + [D_{ov}] \rightarrow [2DH] , \tag{6}$$

where $[D_{ov}]$ is a single oxygen vacancy (orange-orange circles), and $[2DH]$ (orange-blue circles) is considered to be a single defect with two hydrogen bonds. This reaction is illustrated in Fig. 13.

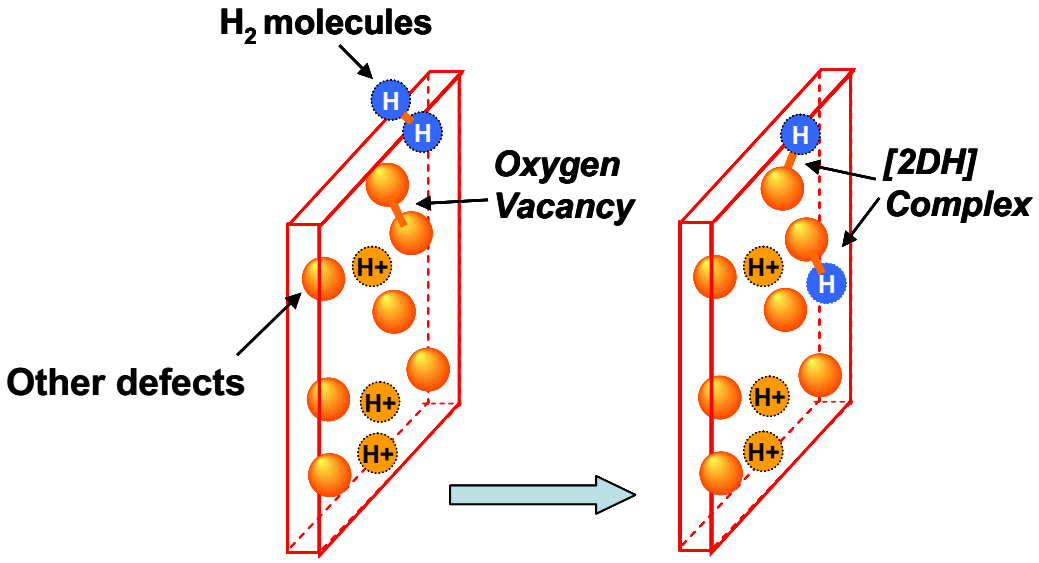


Fig. 13. Cartoon shows the reaction between molecular hydrogen and vacancy defects in the oxide.

Using the above model, the process of H_2-enhanced interface trap buildup was modeled in COMSOL Multiphysics, a finite element simulator. The simulation incorporates carrier drift and diffusion, electrostatics, H_2 diffusion, and chemical reactions of H_2 cracking at oxygen vacancies, proton generation, and interface state generation. Due to the complexity of the reaction processes, only a steady-state solution was obtained. The COMSOL simulation was performed on a 2-D rectangular SiO_2 structure with a thickness of 1μm, approximately the same oxide thickness as the actual bipolar device used in the experiments. The system of continuity equations used to describe the interface trap formation process includes the Poisson's equation describing electrostatics,

$$\frac{\partial E_{ox}}{\partial x} = \frac{q}{\varepsilon_{ox}}\left(p^{+} - n^{-} + N_{H^{+}}\right), \tag{7}$$

where E_{ox} is the oxide electric field, ε_{ox} is the permittivity of SiO_2, p^+ and n^- are hole and electron concentrations, respectively, and N_{H+} is the proton concentration.

The hole continuity equation describes the generation, drift, diffusion, and reaction processes of radiation-induced holes,

$$\frac{\partial p^{+}}{\partial t} = g_o f_y \dot{R}_D - r_{H^{+},1} p^{+} N_{DH} - r_{H^{+},2} p^{+} N_{DHo} - \frac{\partial f_{p^{+}}}{\partial x}, \tag{8}$$

where $r_{H+,1}$ is the reaction constant for holes reacting with H_2-induced Si-H bonds, $r_{H+,2}$ is the reaction constant for holes reacting with pre-existing Si-H bonds, f_y is the hole yield, and f_{p+} is the hole flux that incorporates both drift and diffusion terms in the simulation. The electron continuity equation is as follows,

$$\frac{\partial n^{-}}{\partial t} = g_o f_y \dot{R}_D - \frac{\partial f_{n^{-}}}{\partial x}. \tag{9}$$

Due to high mobility of electrons (20 $cm^{-2}/(V{\cdot}s)$) in the oxide in comparison to holes (10^{-8}

$cm^{-2}/(V \cdot s)$) [21], and a single dose rate used during simulation, the reactions with electrons were ignored. However, this assumption cannot be used when simulating dose rate dependent effects (such as ELDRS in bipolar devices), because at high dose rates electrons can stay in the oxide for longer times due to the large localized field induced by high space charge (holes) generated at high dose rates.

The formation process also includes the proton generation/transport/reaction equation,

$$\frac{\partial N_{H^+}}{\partial t} = r_{H^+,1} p^+ N_{DH} + r_{H^+,2} p^+ N_{DHo} - \frac{\partial f_{H^+}}{\partial x}, \tag{10}$$

where f_{H+} is the proton flux that includes both drift and diffusion terms, $r_{H+,1}$ and $r_{H+,2}$ are reaction constants identical to those of (8). The proton mobility is estimated to be $\sim 10^{-11}$ $cm^{-2}/(V \cdot s)$) [18], which is three orders of magnitude lower than hole mobility. The diffusivity of protons is calculated using the Einstein relation (same for e/h).

The core of the model includes the reactions of molecular hydrogen with O-vacancies. The continuity equation for H_2 is expressed as

$$\frac{\partial N_{H_2}}{\partial t} = -r_{DH} N_{H_2} (D_{ov} - N_{DH}) - \frac{\partial f_{H_2}}{\partial x}, \tag{11}$$

where r_{DH} is the reaction rate for the H_2 cracking reaction, D_{ov} is the density of O-vacancies, N_{DH} is the density of [2DH] in (6), and f_{H2} is the diffusive flux of H_2 in the oxide. The model treats N_{DH} as a non-transporting defect. It is governed by its generation and annihilation reactions,

$$\frac{\partial N_{DH}}{\partial t} = -r_{H^+} p^+ N_{DH} + r_{DH} N_{H_2} (D_{ov} - N_{DH}). \tag{12}$$

The last equation for the model captures the generation of interface traps at the Si/SiO_2 interface, which is the same reaction described by the two-stage hydrogen model with the assumptions of no saturation and annealing,

$$\frac{\partial N_{it}}{\partial t} = N_{Si-H} \sigma_{it} f_{H^+}. \tag{13}$$

The 2-D simulation was performed for hydrogen concentrations from 10^{18} cm^{-3} (100%) to 10^{11} cm^{-3} (0.0001%) in decade intervals. The radiation dose rate was 20 rad/s, and the steady state solution was calculated for a total dose of 30krads, which is the same as the experimental setup.

The simulation results are plotted against the experimental data in Fig. 14. The close match of the simulation with experimental data strongly suggests that H_2 cracking reactions can indeed lead to enhanced interface trap generation in hydrogenated devices. We used some fitting parameters (r_{DH} , N_{DHo}) to exactly match the experimental data.

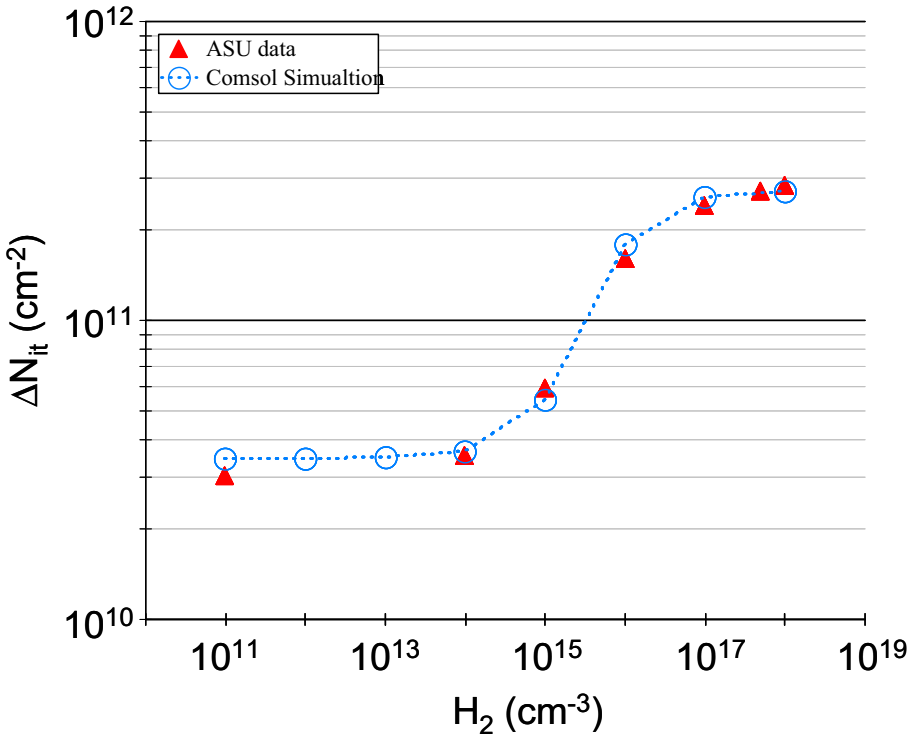


Fig. 14. Comsol Simulation versus ASU Data on the effect of H_2.

3.3 Modeling ELDRS and Effect of Hydrogen on ELDRS

There are several models discussed in physics literature that provide limited description of the mechanisms of ELDRS. Currently, the most popular is the space charge model [17, 22, 23]. The space charge model is directly related to the two-stage hydrogen model of N_{it} formation and trapped-hole model of N_{ot} formation. In this model, due to lower electric fields in bipolar oxides, the space charge generated by radiation (both holes and released protons) transports very slowly in the oxide. At HDRs, the large amount of space charge generated cannot transport quickly to the interface or out of the oxide, thus creating a localized field that retards the transport of other holes and protons to the interface. This subsequently reduces the amount of interface trap and oxide-trapped-charge buildup. At LDRs, the space-charge-induced field is not high enough to reduce the amount of protons and holes reaching the interface, and a higher rate of degradation is observed. Even though the space charge model provides reasonable qualitative explanations for the basic effect, it cannot fully explain the dependence of ELDRS characteristics on the aforementioned factors, particularly the transition dose rates (between low and high dose rate response) in devices that exhibit ELDRS. Indeed, past theoretical/computational treatment of the space charge model have always inadequately described experimental data.

When a silicon-based device with a low externally applied field in the device oxide (such as in a bipolar device) is exposed to uniform ionizing dose exposure, electron/hole pairs are generated uniformly throughout the device oxide. At HDRs, the large buildup of space charge not only builds up localized E-fields to limit the transport of other positively charged species (described as the sole effect in the space charge model), it also stimulates competition of other processes that can reduce the generation of interface traps and

trapped charge. Such processes include free electron/hole recombination, trapped electrons recombining with free holes [24], and free electrons recombining with trapped holes. Reactions with electrons are assumed to be non-existent in the conventional space charge model due to their high mobility (as opposed to holes) in the SiO_2 system. However, because of the high localized E-fields induced at high dose rates, electrons can be confined in the oxide for longer periods. As more electrons are confined in the oxide, the probability of trapping and recombination becomes higher.

The ELDRS model presented here treats electron/hole recombination as a critical mechanism that causes ELDRS. Based on the two-stage, H-transport model, it integrates all of the space charge effects included in the conventional space charge model by solving the Poisson's equation,

$$\frac{\partial E_{ox}}{\partial x} = \frac{q}{\varepsilon_{ox}}(p^+ - n^- + N_{H^+}), \tag{14}$$

in conjunction with hole and electron transport/reaction equations that incorporate all of the electron-hole recombination reactions,

$$\frac{\partial p^+}{\partial t} = g_o \dot{R}_D - \sigma_{recomb} n^- p^+ - r_{H^+} p^+ N_{DHo} - \frac{\partial f_{p^+}}{\partial x}, \tag{15}$$

$$\frac{\partial n^-}{\partial t} = g_o \dot{R}_D - \sigma_{recomb} n^- p^+ - \frac{\partial f_{n^-}}{\partial x}, \tag{16}$$

where R_d is the dose rate, and σ_{recomb} is the electron/hole recombination constant expressed in terms carrier mobilities in the oxide, according to the theory of general ionic recombination [20],

$$\sigma_{recomb} = \frac{q(\mu_n + \mu_p)}{\varepsilon_{ox}}. \tag{17}$$

The subsequent proton generation/transport and interface trap formation processes shares the same basic equations as the hydrogen transport model presented in the last section.

Again using COMSOL multi-physics, 2-D dose rate dependent simulations were carried out on the same structure discussed in the previous section. Because electron trapping is considered unlikely due to very low capture cross-sections in SiO_2 during irradiation, it was omitted in our model simulations. To reduce the complexity of the simulations, all electron recombination reactions were treated as recombination of free electrons and free holes. The model simulations were performed only for interface trap formation because the effect of ELDRS on oxide-trapped-charge buildup was not observed in the experimental data. The simulations were carried out for dose rates from 1mrad/s to 1000 rad/s in decade intervals. Simulations with multiple applied biases were also performed to verify the bias dependence of the ELDRS response. The main simulation results are shown in Fig. 15.

In Fig. 15, the ELDRS characteristics are clearly shown, and the ELDRS effect is noticeably reduced by the applied bias (at the interface). The E-field due to the externally applied bias limits the amount of positively charged protons reaching the interface to form interface traps and, thus, is most significant at low dose rates due to very small localized E-fields in the oxide. The simulation results presented here were not intended to

fit any experimental data. However the results compare well to previously published data on lateral pnp bipolar transistors in Fig. 16 [23].

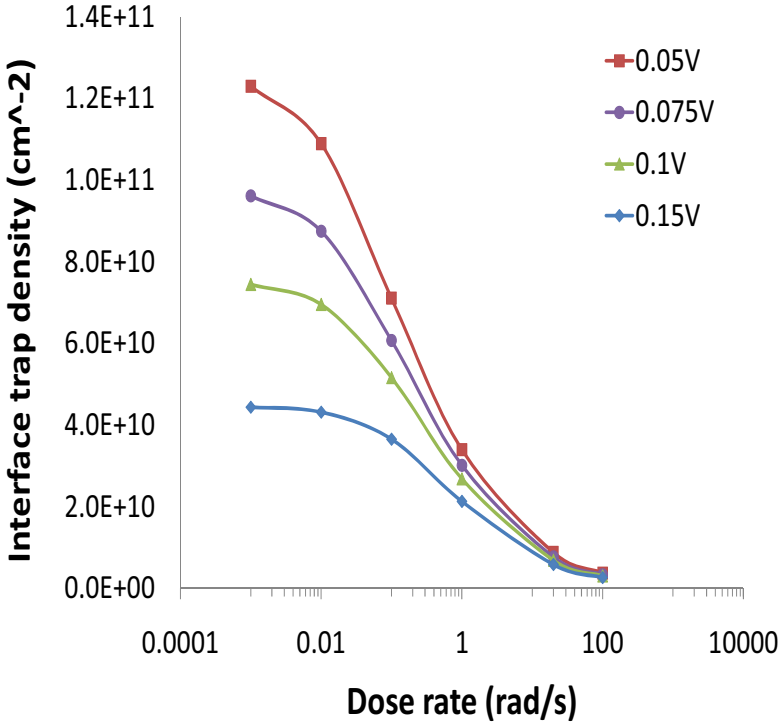


Fig. 15. Simulations of ELDRS model incorporating e/h recombination as a core mechanism. The simulations were performed with several applied bias conditions to show the bias dependence of ELDRS.

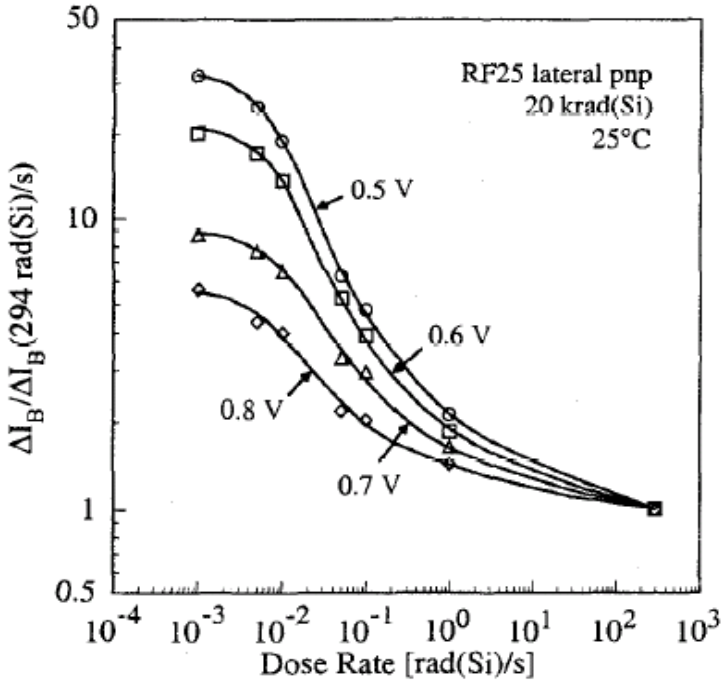


Fig. 16. The dose rate experimental data showing bias dependence of ELDRS response obtained from lateral pnp transistors.

As discussed previously, ELDRS is caused by a combination of space charge effects and competing reactions in the bipolar device oxide. With the addition of hydrogen, H_2 in the case of this study, dramatic differences were observed in the ELDRS characteristics. The effect of hydrogen on ELDRS, conceptually, is fairly straightforward. As more hydrogen is introduced to the device oxide, the reactions of excess hydrogen with radiation-induced charge (H_2 cracking or similar reactions) begin to compete with both space charge effects and other reactions during irradiation. Depicted in Fig. 17 is a device with low hydrogen concentration. The major ELDRS mechanisms are reactions such as electron-hole pair (ehp) recombination.

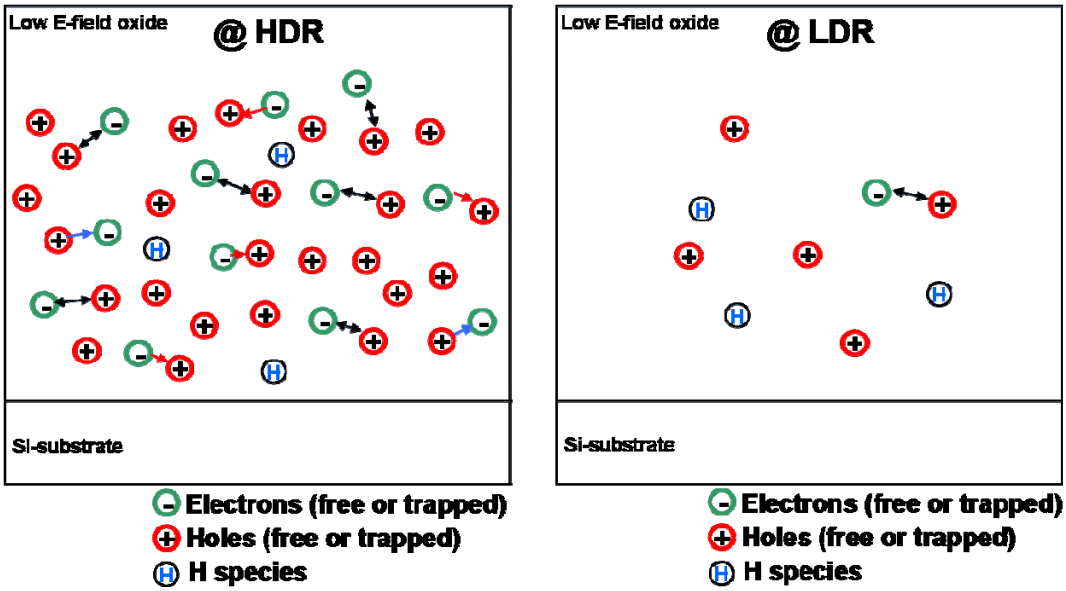


Fig. 17. Conception of core processes in a device exhibiting ELDRS with low hydrogen concentration.

In the hydrogenated device, shown in Fig. 18, the reaction between radiation-induced holes and hydrogen compete with ehp recombination. This competition increases the probability of proton generation (and subsequent N_{it} formation) to various degrees depending on dose rate and can result in shifted characteristics in the ELDRS response.

To model the effect of hydrogen, a simplified approach was taken to account for the competition between hydrogen reactions and electron/hole recombination. In COMSOL, the coefficient of ehp recombination (σ_{recomb}) was modeled as an inverse function of hydrogen concentration:

$$\sigma_{rcomb} \propto \frac{\partial \sigma_{rcomb,o}}{\left[N_{DH}(H_2)\right]^{\beta}}, \tag{18}$$

where N_{DH} is the density of hydrogen complexes generated by H_2, α and β are arbitrary fitting constants, and $\sigma_{recomb,o}$ is the low-hydrogen recombination coefficient.

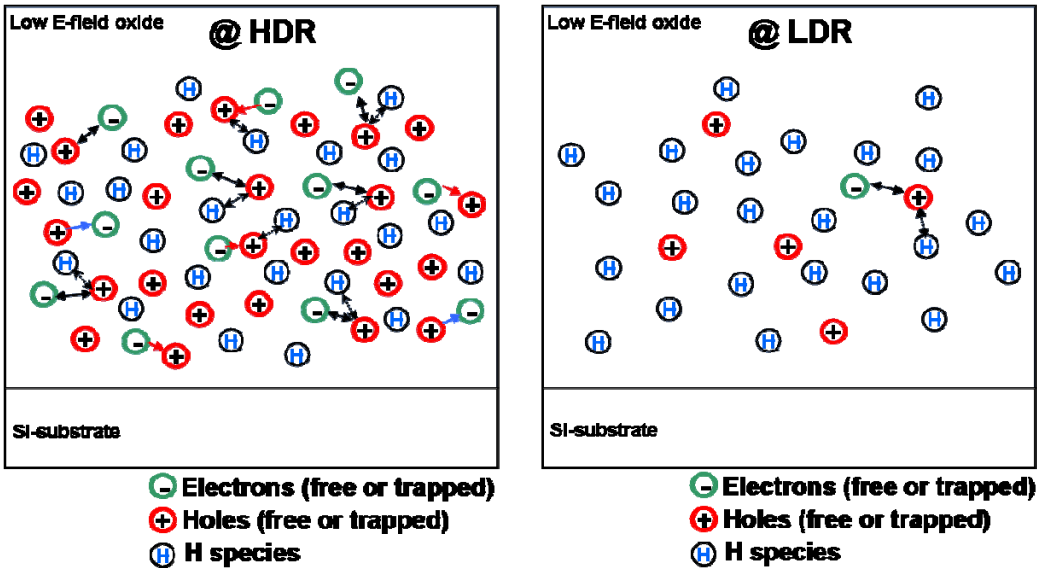


Fig. 18. Conception of core processes in a device exhibiting ELDRS with high hydrogen concentration.

3.4 Simulation Results Using COMSOL

The hydrogen species in the oxide was simply modeled as a combination of pre-existing and H_2-induced hydrogen complexes. In this modeling approach, as hydrogen concentration increases, the probability of ehp recombination reduces, and more protons can be generated from reactions between holes and hydrogen complexes to form interface traps. Furthermore, the boundary condition at the Si/SiO_2 interface was modeled differently. Instead of allowing protons to cross the interface easily (setting proton concentration to be zero at the interface), as what was modeled in TID simulations, the proton flux was set to zero at the interfacial boundary to not allow any to escape into the silicon. This approach is more realistic physically because there is a large energy barrier for protons to enter the silicon according to quantum mechanical calculations [25]. The simulation results are shown in Fig. 19.

The preliminary results in Fig. 19 shows that as the hydrogen concentration is increased from DH4 to DH1, the ELDRS transition region shifts to higher dose rates. In addition, the low dose rate saturation limit also increases. These results clearly show excellent qualitative agreement with the experimental data.

Even though ASU's COMSOL model is not yet designed to fit experimental data, it was able to capture the essential mechanism of ELDRS and the effect of hydrogen on ELDRS described in this report. That is, the dose rate response in bipolar ICs is governed by the competing processes of carrier recombination, and hydrogen reactions as well as space charge effects.

Modeling the effect of hydrogen has so far focused mainly on the formation of interface traps. One major omission in the model is the formation of trapped charge in the oxide and its effect on the transport of charged species such as free protons and holes. In the next phase of the modeling work, charge trapping and its influence on oxide field will be included. This will provide a more accurate description of the processes that influence the TID and dose rate response of bipolar ICs.

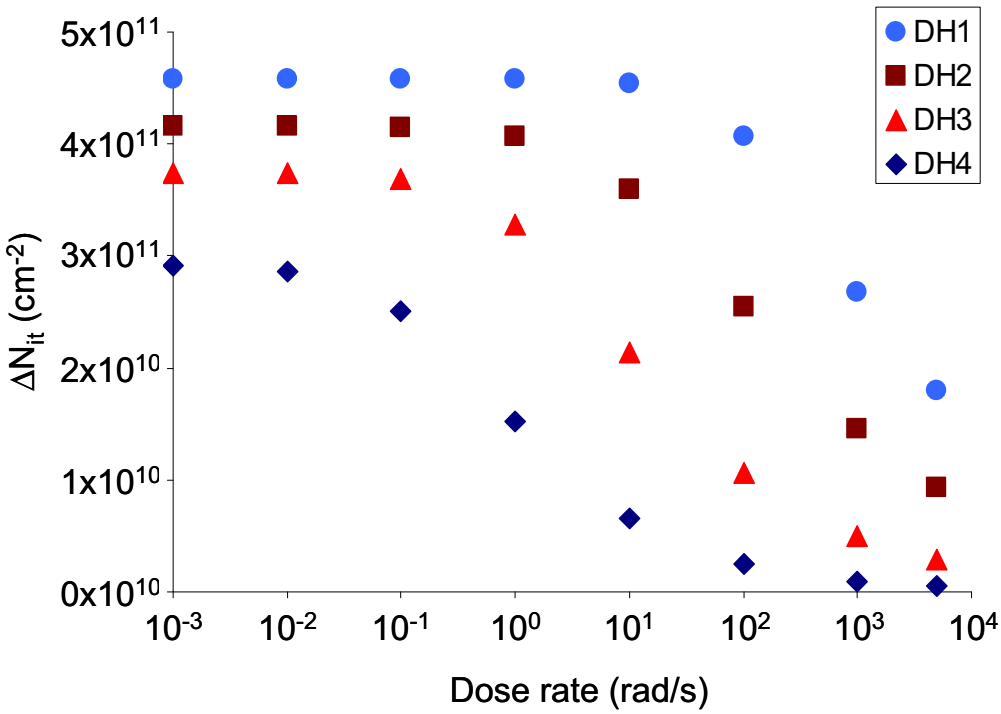


Fig. 19. Simulation of the effect of hydrogen on ELDRS response: right shift of transition dose rates and increase of low dose rate saturation limit.

4.0 CONCLUSIONS AND IMPLICATIONS

ELDRS in bipolar linear circuits has been a major topic of research since it was first reported [3]–[6]. Early test results and modeling seemed to indicate that the phenomenon of ELDRS was a result of the processing and thickness of the base oxide. Later studies have shown that the dominate factors that determine total dose response and ELDRS are the final passivation [9]–[11], the packaging and post packaging thermal treatments [12], and the amount of hydrogen that may be trapped in the package [13]–[15]. Certain types of final passivation may introduce large amounts of hydrogen into the base oxide, such as the low temperature nitride process which uses ammonia and silane. Thermal treatments can both drive the hydrogen into the base oxide and alter the means by which the hydrogen is incorporated in the oxide. Moreover, external sources of hydrogen can rapidly diffuse through intervening passivation layers into the base oxide [13] unless there is a barrier such as nitride [14].

Because hydrogen appears to be a dominant factor determining both the total dose and dose rate responses of linear bipolar circuits, we have conducted experiments on both transistor structures and linear circuits to measure this response as a function of the externally introduced hydrogen concentration. The results of these experiments show that a greater amount of hydrogen does two things: it increases the degradation at low dose rate and it increases the dose rates region where the transition from high dose rate to low dose rate enhancement occurs. The mechanisms for these trends were explored with a code that incorporates the basic drift-diffusion equations as well as kinetic equations for hydrogen cracking and free electron hole recombination. The results from this model indicate that the saturation at low dose rate (also observed experimentally in this document or previously [26-27]) is increased with H_2. Further experiments at a lower dose rate will be needed to completely validate these results.

There are a number of implications of this research:

1. The bipolar linear circuits should be processed and packaged with a minimum amount of hydrogen to achieve reasonable total dose hardness and minimize ELDRS. If the amount of hydrogen introduced during processing through metallization ensures an acceptable response, then the post metal processes should be designed to minimize any further introduction of hydrogen.
2. If the amount of hydrogen, both initially in the base oxide and introduced after metallization is low, then the transition to ELDRS may occur at a very low dose rate. An example of this can be seen in Figs. 8 and 9 for the “virgin” LM193. Therefore, some parts that have only been tested at dose rates as low as 10 mrad/s may show enhanced degradation when taken to even lower dose rates. Experiments are underway to explore this possibility. If this turns out to be the case, it would have severe implications for MIL-STD-883, Test Method 1019.
3. An accelerated hardness assurance test method may be possible by testing parts at high dose rate (100 rad/s) in a 100% H_2 atmosphere to set an upper bound to the low dose rate response in space [2]. The technique is to irradiate parts with package lids removed in a glass tube pressurized with 100% H_2. Parts with nitride will prevent any penetration of externally applied hydrogen. To use this approach the nitride would have to be removed. This approach has only been demonstrated on a gated lateral pnp test transistor (glpnp) and one circuit type. Experiments

have been proposed to investigate this approach on a wide variety of ELDRS part types. Fig. 20 shows the comparison of degradation at low dose rate with no applied hydrogen to irradiation at high dose rate in 100% H_2.While such an approach may work for many part types, especially those with total dose response dominated by lateral and substrate pnps, it may not work for those parts dominated by npn transistors or parts with a nitride passivation [11].

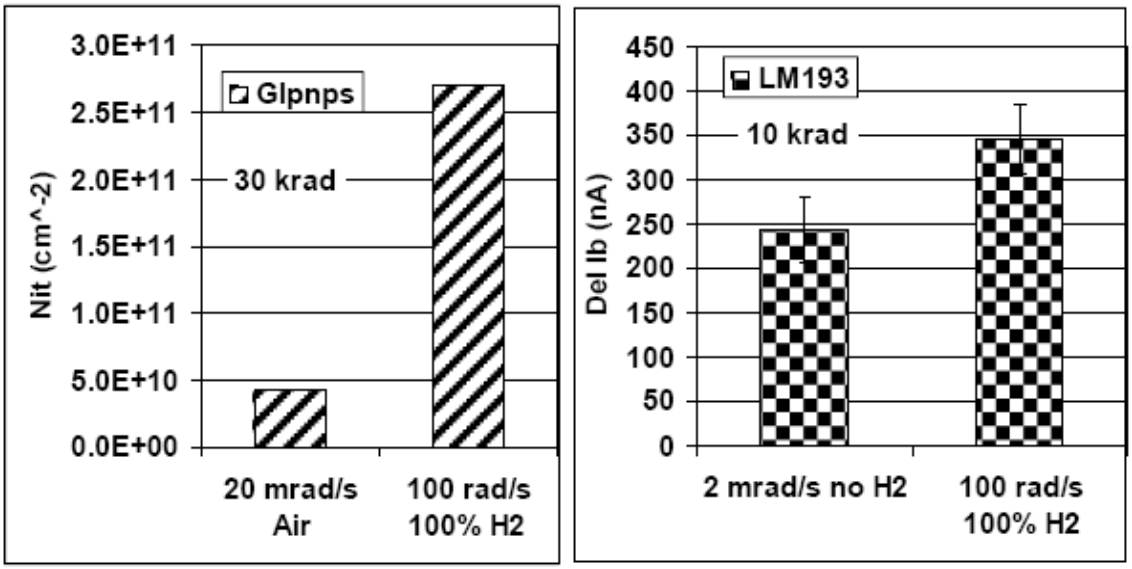


Fig. 20. Comparison of post irradiation N_{it} for a glpnp irradiated to 30 krad(Si) at 20 mrad(Si)/s in air to irradiation at 100 rad(Si)/s in 100% H_2 (left) and delta Ib of an LM193 to 10 krad(Si) at 2 mrad(Si)/s in air to irradiation at 100 rad(Si)/s in 100% H_2 (right).

5.0 REFERENCES

[1] E. Nicollian and J. Brews, *MOS (Metal Oxide Semiconductor Physics and Technology)*. NY: John Wiley & Sons, 1982.

[2] R. K. Lowry, "Sources of Volatile Gases Hazardous to Hermetic Electronic Enclosures," *IEEE Trans. Elec. Packaging Man.,* vol. 22, pp. 319–323, 1999.

[3] Enlow, E. W., R. L. Pease, W. E. Combs, R. D. Schrimpf, and R. N. Nowlin, "Response of Advanced Bipolar Processes to Ionizing Radiation," *IEEE Trans. Nuc. Sci.* NS-38, No.6, 1342–1351, December 1991.

[4] McClure, S., R. L. Pease, W. Will, and G. Perry, "Dependence of Total Dose Response of Bipolar Linear Microcircuits on Applied Dose Rate," *IEEE Trans. Nuc. Sci.* NS-41, No.6, 2544–2549, December 1994.

[5] Johnston, A. H, G. M. Swift, and B. G. Rax, "Total Dose Effects in Conventional Bipolar Transistors and Linear Integrated Circuits," *IEEE Trans. Nuc. Sci.* NS-41, No.6, 2427–2436, December 1994.

[6] Pease, R. L., J. F. Krieg, T. L. Turflinger, A. B. Campbell, and R. J. Walters, "Recent data from From the MPTB ELDRS in Space, submitted to *Journal of Radiation Effects: Research and Engineering*, 2003.

[7] Turflinger, T. L., W. M. Schemichel, J. F. Krieg, J. L. Titus, A. B. Campbell, M. Reeves, R. J. Walters, P. W. Marshall, and R. L. Pease, "ELDRS in Space: An Updated and Expanded Analysis of the Bipolar ELDRS on MPTB," *IEEE Trans. Nucl. Sci.* NS-50, No.6, 2328–2334, December 2003.

[8] Beaucour, J. T., T. Carriere, A. Gach, D. Laxague, and P. Poirot, "Total Dose Effects on Negative Voltage Regulator," *IEEE Trans. Nuc. Sci.* NS-41, No.6, 2420–2426, December 1994.

[9] Pease, R. L., D. G. Platteter, G. W. Dunham, J. E. Seiler, H. J. Barnaby, R. D. Schrimpf, M. R. Shaneyfelt, M. C. Maher, and R. N. Nowlin, "Characterization of Enhanced Low Dose Rate Sensitivity (ELDRS) Effects Using Gated Lateral PNP Transistor Structures," *IEEE Trans. Nucl. Sci.* NS-51, No.6, 3773–3780, December 2004.

[10] Shaneyfelt, M. R., R. L. Pease, J. R. Schwank, M. C. Maher, G. L. Hash, D. M. Fleetwood, P. E. Dodd, C. A. Reber, S. C. Witczak, L. C. Riewe, H. P. Hjalmarson, J. C. Banks, B. L. Doyle, and J. A. Knapp, "Impact of Passivation Layers on Enhanced Low-Dose-Rate Sensitivity and Thermal-Stress Effects in Linear Bipolar ICs," *IEEE Trans. Nucl. Sci.* NS-49, No.6, 3171–3179, December 2002.

[11] Seiler, J. E., D. G. Platteter, G. W. Dunham, R. L. Pease, M. C. Maher, and M. R. Shaneyfelt, "Effects of passivation on the enhanced low dose rate sensitivity of National LM124 operational amplifiers," IEEE Radiation Effects Data Workshop Record, p. 42, 2004.

[12] Shaneyfelt, M. R., J. R. Witczak, J. R. Schwank, D. M. Fleetwood, R. L. Pease, P. S. Winokur, L. C. Riewe, and G. L. Hash, "Thermal-Stress Effects on Enhanced

Low Dose Rate Sensitivity in Linear Bipolar ICs," *IEEE Trans. Nucl. Sci.* NS-47, No.6, 2539–2545, December 2000.

[13] Chen, X. J., H. Barnaby, B. Vermeire, R. Pease, D. Platteter, G. Dunham, J. Seiler, and S. McClure, "Mechanisms of enhanced radiation-induced degradation due to excess molecular hydrogen in bipolar oxides," *IEEE Trans. Nucl. Sci.* NS-54, No.6, 1913–1919 December 2007.

[14] Adell, P. C., S. McClure, R. L. Pease, B. G. Rax, G. W. Dunham, H. J. Barnaby, and X. J. Chen, "Impact of hydrogen contamination on the total dose response of linear bipolar microcircuits," presented at RADECS, Deauville, France, September, 2007.

[15] Pease, R. L, M. C. Maher, M. R. Shaneyfelt, M. Savage, P. Baker, J. Krieg, and T. Turflinger, "Total dose hardening of a bipolar voltage comparator," *IEEE Trans. Nucl. Sci.* NS-49, No. 6, 3180–3184, December 2002.

[16] Chen, X. J., H. J. Barnaby, R. L. Pease, R. D. Schrimpf, D. Platteter, M. Shaneyfelt, and B. Vermiere, "Estimation and Verification of Radiation Induced Not and Nit Energy Distribution Using Combined Bipolar and MOS Characterization Methods in Gated Bipolar Devices," *IEEE Trans Nucl. Sci.,* vol. 52, 2005.

[17] McLean, F. B., "A framework for understanding radiation-induced interface states in SiO_2," *IEEE Trans. Nucl. Sci.,* vol. 27, pp. 1651–1657, 1980.

[18] Rashkeev, S. N., C. R. Cirba, D. M. Fleetwood, R. D. Schrimpf, S. C. Witczak, A. Michez, and S. T. Pantelides, "Physical model for enhanced interface trap formation at low dose rates," *IEEE Trans. Nucl. Sci.,* vol. 49, pp. 2650–2655, 2002.

[19] Winokur, P. S., and J. H. E. Boesch, "Interface-state generation in radiation-hard oxides," *IEEE Trans. Nucl. Sci.,* vol. 27, p. 1647, 1980.

[20] Batyrev, I. G., D. R. Hughart, B. Tuttle, M. Bounasser, R. D. Schrimpf, M. Law, D. M. Fleetwood, and S. T. Pantelides, "Mechanisms of Hydrogen Effects in Bipolar Radiation Response," presented at NSREC'08 Tucson, Arizona, 2008.

[21] Muller, R. S., and T. I. Kamins, *Device Electronics for Integrated Circuits*, Second ed. New York: Wiley, 1986.

[22] Fleetwood, D. M., S. L. Kosier, R. N. Nowlin, R. D. Schrimpf, R. A. Reber, M. Delaus, P. S. Winokur, A. Wei, W. E. Combs, and R. L. Pease, "Physical mechanisms contributing to enhanced bipolar gain degradation at low dose rates," *IEEE Trans. Nucl. Sci.,* vol. 41, pp. 1871–1883, 1994.

[23] Witczak, S. C., R. C. Lacoe, D. C. Mayer, D. M. Fleetwood, R. D. Schrimpf, and K. F. Galloway, "Space charge limited degradation of bipolar oxide at low electric fields," *IEEE Trans. Nucl. Sci.,* vol. 45, pp. 2339–2351, 1998.

[24] Boch, J., F. Saign, R. D. Schrimpf, J.-R. Vaill, L. Dusseau, and E. Lorfvre, "Physical Model for the Low-Dose Rate Effect in Bipolar Devices," *IEEE Trans. Nucl. Sci.,* vol. 53, pp. 3655–3660, 2006.

[25] Rashkeev, S. N., D. M. Fleetwood, R. D. Schrimpf, and S. T. Pantelides, "Effects of Hydrogen Motion on Interface Trap Formation and Annealing," *IEEE Trans Nucl. Sci.,* vol. 51, p. 3158, 2004.

[26] Pease, R. L., "Total-dose issues for microelectronics in space systems," *IEEE Trans. Nucl. Sci.*, vol 43, pp. 442–452, 1996.

[27] Pease, R. L., R. D. Schrimpf, and D. M. Fleetwood, "ELDRS in Bipolar Linear Circuits: A review," Accepted for publication in *IEEE Trans. Nucl. Sci*.